Received: 20 October 2018

DOI: 10.1002/mma.6259

RESEARCH ARTICLE

WILEY

Spatiotemporal patterns induced by delay and cross-fractional diffusion in a predator-prey model describing intraguild predation

Zhan-Ping Ma[1] | **Hai-Feng Huo**[2] | **Hong Xiang**[2]

[1]School of Mathematics and Information Science, Henan Polytechnic University, Jiaozuo, 454003, Henan, People's Republic of China

[2]Department of Applied Mathematics, Lanzhou University of Technology, Lanzhou, 730050, Gansu, People's Republic of China

Correspondence
Hai-Feng Huo, Department of Applied Mathematics, Lanzhou University of Technology, Lanzhou, Gansu 730050, People's Republic of China.
Email: hfhuo@lut.cn

Communicated by: M. Efendiev

In this article, we study a reaction-diffusion predator-prey model that describes intraguild predation. We mainly consider the effects of time delay and cross-fractional diffusion on dynamical behavior. By using delay as the bifurcation parameter, we perform a detailed Hopf bifurcation analysis and derive the algorithm for determining the direction and stability of the bifurcating periodic solutions. We also demonstrate that proper cross-fractional diffusion can induce Turing pattern, and the smaller the order of fractional diffusion is, the more easily Turing pattern is able to occur.

KEYWORDS

cross-fractional diffusion, delay, Hopf bifurcation, predator-prey, Turing pattern

MSC CLASSIFICATION

35K57; 35B32; 92D25

1 | INTRODUCTION

Omnivory, as defined in Pimm and Lawton,[1] occurs when a population feeds on resources at more than one trophic level. An example of this is the so-called intraguild predation (IGP). IGP is the killing and eating of prey species by a predator that also can utilize the resources of those prey.[2] There has been numerous biological evidence showing that IGP is a widespread interaction within natural communities.[3,4] Since the pioneering work of Polis et al,[2,5] a great deal of research have been devoted to the study of IGP models, and lots of interesting dynamical phenomena, such as limit cycles, bistability, bifurcation, and chaos, have been uncovered.[3,4,6,7]

One of the mathematical model describing IGP was developed by Holt and Polis.[8] Their model takes the following form:

$$\begin{cases} \frac{du}{dt} = u\left(\frac{be}{cv+eu} - dv - m\right), \\ \frac{dv}{dt} = v\left(\frac{bc}{cv+eu} + du - n\right). \end{cases} \tag{1}$$

Here, $u(t)$ and $u(t)$ stand for the density of prey and predator, respectively. c, e are the parameters denoting the consumption of the predator and the prey species for the common resources. The ratio $\frac{e}{c}$ measures the relative abilities of the two species to compete for the common resources. d is the predation rate. m, n are the natural death rates of the prey and the predator, respectively. b is scaling parameter. In the dynamics of real populations, the reproduction of predator after consuming the prey is not instantaneous, but is mediated by some reaction-time lags required for gestation. It has been shown that such time delays can destabilize an otherwise stable steady state and induce oscillations in predator-prey model.[9-12] On the contrary, similar delays do not cause sustained oscillations in competition models with monotone

response functions.[13] It is worth noting that IGP models involve both predator-prey interactions and competition. Consequently, it is of great interest to investigate the dynamics of the system (1) when delay is presented. In nature, species are spatially heterogeneous, and individuals will tend to migrate towards regions of lower population density to increase the possibility of survival,[14] and hence species are distributed over space and interact with each other within their spatial domain. For this reason, we consider the following model in a bounded domain $\Omega \subset \mathbb{R}^N$ with no-flux boundary condition:

$$\begin{cases} \frac{\partial u}{\partial t} - d_1 \Delta u = u\left(\frac{be}{cv+eu} - dv - m\right), & (x,t) \in \Omega \times (0,\ \infty), \\ \frac{\partial v}{\partial t} - d_2 \Delta v = v\left(\frac{bc}{cv+eu} + du(x,t-\tau) - n\right), & (x,t) \in \Omega \times (0,\ \infty), \\ \frac{\partial u}{\partial \nu} = \frac{\partial v}{\partial \nu} = 0, & (x,t) \in \partial\Omega \times (0,\ \infty), \\ u(x,0) = u_0(x) \geq 0,\ v(x,0) = v_0(x) \geq 0, & x \in \overline{\Omega} \times [-\tau, 0], \end{cases} \tag{2}$$

where $\Omega \subset \mathbb{R}^N$ is a bounded domain with smooth boundary $\partial\Omega$ and ν is the outward unit normal on $\partial\Omega$. The no-flux boundary condition indicates that there is zero population flux across the boundary. $\tau \geq 0$ represents the gestation time of the predator. System (2) has a positive constant steady state if and only if

$$\frac{n}{c} > \frac{m}{e} \text{ and } \frac{n}{d} > \frac{bc}{en - cm} > \frac{m}{d}, \tag{3}$$

in which case, it is uniquely given by

$$u^* = \frac{n}{d} - \frac{bc}{en - cm},\ v^* = -\frac{m}{d} + \frac{be}{en - cm}.$$

Fang and Wang[6] proved that the positive constant steady state (u^*, v^*) of system (2) is globally asymptotically stable when $\tau = 0$, which implies that there is no spatiotemporal patterns for system (2) with $\tau = 0$. In the past decades, spatiotemporal dynamic patterns, especially in biology, mathematical ecology, and chemistry, have been investigated widely by many authors.[15-27] Currently, the spatiotemporal patterns of population distribution have been a hot topic because species abundance changes not only in time but also in space. Our first objective is to show that delay can induce spatially homogeneous and inhomogeneous periodic oscillatory patterns resulting from Hopf bifurcation.

The groundbreaking discoveries of Turing[28] suggested that diffusion in a mixture of chemically reacting species could cause instability of a spatially uniform state, leading to the formation of spatial patterns. Later, spontaneous formation was observed in the 1990s in controlled laboratory experiments.[29,30] Now, Turing mechanism has been extensively accepted and studied in diverse disciplines. However, system (2) with $\tau = 0$ has no Turing pattern, ie, self diffusion does not trigger the Turing pattern. This mainly motivated us to consider the anomalous diffusion in system (2) with $\tau = 0$. Anomalous diffusion can be understood by considering a random walk with Lévy flights.[31] The important consequence of having a Lévy distribution of step lengths that is asymmetric in general is that the corresponding diffusion equation contains fractional derivatives, instead of the Laplacian operator.[32] In the context of population dynamics, anomalous diffusion (rather than classical diffusion) has been employed as a more appropriate way to describe the motion of animals under certain circumstances.[33-35] Taking into account the movement of the species with Lévy flight type and the dispersal of the species, it is known that the movement of the species is influenced by its interacting species, which is usually referred to as cross diffusion. We consider the following cross-fractional diffusion system:

$$\begin{cases} \frac{\partial u}{\partial t} = d_1 \nabla^\gamma u - d_{12} \nabla^\gamma v + u\left(\frac{be}{cv+eu} - dv - m\right), \\ \frac{\partial v}{\partial t} = d_{21} \nabla^\gamma u - d_2 \nabla^\gamma v + v\left(\frac{bc}{cv+eu} + du - n\right). \end{cases} \tag{4}$$

Here, d_1 and d_2 are the self-fractional diffusive coefficients. d_{12} and d_{21} are the cross-fractional diffusive coefficients. $\nabla^\gamma (1 < \gamma < 2)$ is a fractional power Laplacian, and

$$\nabla^\gamma U = -\frac{\sec(\pi\gamma/2)}{2\Gamma(2-\gamma)} \frac{d^2}{dx^2} \int_{-\infty}^{+\infty} \frac{U(y)}{|x-y|^{\gamma-1}} dy.$$

$1 < \gamma < 2$ and $0 < \gamma < 1$ correspond to a Lévy super-diffusion and sub-diffusion, respectively. We consider an especially interesting case of super-diffusion, Lévy flights. In the context of population dynamics, super-diffusion (rather than classical diffusion) has been employed as a more appropriate way to describe the motion of animals under certain circumstances.[34]

Our second goal is to study the effect of cross-fractional diffusion on system (4). We will show that self fraction diffusion ($d_{12} = d_{21} = 0$) still cannot create Turing pattern. But when cross-fractional diffusion coefficients d_{12} and d_{21} fall into some region, Turing pattern can occur (see Theorem 5).

The rest of the paper is organized as follows. In Section 2, we give conditions on the stability of the positive constant steady state (u^*, v^*) and the existence of Hopf bifurcation for system (2). In Section 3, by applying the normal form theory and center manifold reduction of partial fractional differential equations (PFDEs),[14] an explicit algorithm for determining the direction and stability of Hopf bifurcation is given. In Section 4, we perform the cross-fractional diffusion–driven instability of the positive constant steady state (u^*, v^*) in system (4). Finally, some numerical simulations and computations are included to support our theoretical results in Section 5, and a brief conclusion is given in Section 6.

2 | STABILITY AND HOPF BIFURCATION

In this section, we consider stability and Hopf bifurcation of system (2) by regarding τ as the bifurcation parameter. In the remainder of this paper, without of loss of generality, we choose the domain $\Omega = (0, l\pi)$ $(l > 0)$ as the spatial domain for simplicity of notations in computing the normal forms and for convenience of carrying out demonstrating numerical results. From the properties of the Laplacian operator defined on the bounded domain, the operator on X has the eigenvalues $\frac{-k^2}{l^2}$ with the relative eigenfunctions

$$\beta_k^1 = \begin{pmatrix} \cos\frac{kx}{l} \\ 0 \end{pmatrix},\ \beta_k^2 = \begin{pmatrix} 0 \\ \cos\frac{kx}{l} \end{pmatrix},\ k \in \mathbb{N}_0 := \{0, 1, 2, \dots\},$$

where

$$X = \left\{ u, v \in W^{2,2}(\Omega) :\ \frac{\partial u(x,t)}{\partial x} = \frac{\partial v(x,t)}{\partial x} = 0,\ x = 0,\ l\pi \right\}.$$

Let $\widetilde{u} = u - u^*, \widetilde{v} = v - v^*$ and drop the tildes for the sake of simplicity. System (2) can be rewritten as

$$\begin{cases} \frac{\partial u}{\partial t} - d_1\Delta u = (u+u^*)\left(\frac{be}{c(v+v^*)+e(u+u^*)} - d(v+v^*) - m\right), & (x,t) \in \Omega \times (0,\ \infty), \\ \frac{\partial v}{\partial t} - d_2\Delta v = (v+v^*)\left(\frac{bc}{c(v+v^*)+e(u+u^*)} + d\,(u(x,t-\tau)+u^*) - n\right), & (x,t) \in \Omega \times (0,\ \infty), \\ \frac{\partial u}{\partial v} = \frac{\partial v}{\partial v} = 0, & (x,t) \in \partial\Omega \times (0,\ \infty), \\ u(x,0) = u_0(x) - u^*,\ v(x,0) = v_0(x) - v^*,\ (x,t) \in \overline{\Omega} \times [-\tau, 0]. \end{cases} \tag{5}$$

The positive constant steady state (u^*, v^*) in system (2) is transformed into $(0, 0)$ steady state of (5). Let

$$f^{(1)}(u,v) = (u+u^*)\left(\frac{be}{c(v+v^*)+e(u+u^*)} - d(v+v^*) - m\right),$$
$$f^{(2)}(u,v,w) = (v+v^*)\left(\frac{bc}{c(v+v^*)+e(u+u^*)} + d(w+u^*) - n\right).$$

Define $f_{ij}^{(1)}$ $(i+j \geq 1)$ and $f_{ijp}^{(2)}$ $(i+j+p \geq 1)$ as follows:

$$f_{ij}^{(1)} = \frac{\partial^{i+j} f^{(1)}(0,0)}{\partial u^j \partial v^j},\ f_{ijp}^{(2)} = \frac{\partial^{i+j+p} f^{(2)}(0,0,0)}{\partial u^j \partial v^j \partial w^p}.$$

In particular,

$$\alpha_1 = f_{10}^{(1)} = -\frac{be^2u^*}{(eu^*+cv^*)^2} < 0,\ \alpha_2 = f_{01}^{(1)} = -u^*\left[\frac{bce}{(eu^*+cv^*)^2} + d\right] < 0,$$
$$\beta_1 = f_{100}^{(2)} = -\frac{bcev^*}{(eu^*+cv^*)^2} < 0,\ \beta_2 = f_{010}^{(2)} = -\frac{bc^2v^*}{(eu^*+cv^*)^2} < 0,\ \beta_3 = f_{001}^{(2)} = dv^* > 0.$$

By Taylor expansion, Equation (5) becomes

$$\begin{cases} \frac{\partial u}{\partial t} - d_1\Delta u = \alpha_1 u + \alpha_2 v + \sum\limits_{i+j\geq 2} \frac{1}{i!j!} f_{ij}^{(1)} u^j v^j, \\ \frac{\partial v}{\partial t} - d_2\Delta v = \beta_1 u + \beta_2 v + \beta_3 u(x,t-\tau) \\ \qquad + \sum\limits_{i+j+p\geq 2} \frac{1}{i!j!p!} f_{ijp}^{(2)} u^j(x,t) v^j(x,t) u^p(x,t-\tau). \end{cases} \tag{6}$$

Denote $u_1(t) = u(\cdot,t)$, $u_2(t) = v(\cdot,t)$ and $U = (u_1,u_2)^T$. Then, (6) can be rewritten as an abstract differential equation in the phase space $\mathcal{C} = C([-\tau,0],X)$,

$$\frac{dU(t)}{dt} = D\Delta U(t) + L(U_t) + F(U_t), \tag{7}$$

where $D = \operatorname{diag}\{d_1,d_2\}$, $\Delta = \operatorname{diag}\left\{\partial^2/\partial x^2, \partial^2/\partial x^2\right\}$, $L : \mathcal{C} \to X$ and $F : \mathcal{C} \to X$ are given, respectively, by

$$L(\varphi) = \begin{pmatrix} \alpha_1\varphi_1(0) + \alpha_2\varphi_2(0) \\ \beta_1\varphi_1(0) + \beta_2\varphi_2(0) + \beta_3\varphi_1(-\tau) \end{pmatrix}$$

and

$$F(\varphi) = \begin{pmatrix} \sum\limits_{i+j\geq 2} \frac{1}{i!j!} f_{ij}^{(1)} \varphi_1^i(0)\varphi_2^j(0) \\ \sum\limits_{i+j+p\geq 2} \frac{1}{i!j!p!} f_{ijp}^{(2)} \varphi_1^i(0)\varphi_2^j(0)\varphi_1^p(-\tau) \end{pmatrix}$$

for $\varphi = (\varphi_1,\varphi_2)^T \in \mathcal{C}$.

It is easy to show that the characteristic equation of the linearization of (7) is equivalent to the sequence of the transcendental equations

$$\lambda^2 + A_k\lambda + B_k + Ce^{-\lambda\tau} = 0,\ k \in \mathbb{N}_0, \tag{8}$$

where

$$A_k = (d_1+d_2)\left(\frac{k}{l}\right)^2 - \alpha_1 - \beta_2 > 0,$$
$$B_k = \left(d_1\left(\frac{k}{l}\right)^2 - \alpha_1\right)\left(d_2\left(\frac{k}{l}\right)^2 - \beta_2\right) - \alpha_2\beta_1,$$
$$C = -\alpha_2\beta_3 > 0.$$

Set

$$\Delta_k(\lambda,\tau) = \lambda^2 + A_k\lambda + B_k + Ce^{-\lambda\tau}. \tag{9}$$

$\lambda = 0$ is not the root of (8), and Bogdanov-Takens singularity does not occur.

Let $\lambda = i\omega$ ($\omega > 0$) be a purely imaginary root of (8) for $k \in \mathbb{N}_0$. Then, we have

$$-\omega^2 + A_k\omega i + B_k + C(\cos\omega\tau - i\sin\omega\tau) = 0.$$

Separating the real and imaginary parts in the above equation, we have

$$\begin{cases} \omega^2 - B_k = C\cos\omega\tau, \\ A_k\omega - C\sin\omega\tau = 0. \end{cases} \tag{10}$$

From (10), we have

$$\omega^4 + \left(A_k^2 - 2B_k\right)\omega^2 + B_k^2 - C^2 = 0, \tag{11}$$

where

$$\begin{aligned} A_k^2 - 2B_k &= \left(d_1^2 + d_2^2\right)\left(\frac{k}{l}\right)^4 - 2\left(d_1\alpha_1 + d_2\beta_2\right)\left(\frac{k}{l}\right)^2 + \alpha_1^2 + \beta_2^2 + 2\alpha_2\beta_1 > 0, \\ B_k^2 - C^2 &= \left(B_k + C\right)\left(B_k - C\right) \\ &= \left[d_1 d_2\left(\frac{k}{l}\right)^4 - \left(d_1\beta_2 + d_2\alpha_1\right)\left(\frac{k}{l}\right)^2 + du^* v^*\right] \cdot \\ &\quad \left[d_1 d_2\left(\frac{k}{l}\right)^4 - \left(d_1\beta_2 + d_2\alpha_1\right)\left(\frac{k}{l}\right)^2 + \alpha_1\beta_2 + \alpha_2(\beta_3 - \beta_1)\right]. \end{aligned}$$

Clearly, $B_k + C > 0$. Set $z = \omega^2$, and (11) is transformed into

$$z^2 + \left(A_k^2 - 2B_k\right)z + B_k^2 - C^2 = 0. \tag{12}$$

If $d_1 d_2\left(\frac{k}{l}\right)^4 - \left(d_1\beta_2 + d_2\alpha_1\right)\left(\frac{k}{l}\right)^2 + \alpha_1\beta_2 + \alpha_2(\beta_3 - \beta_1) < 0$, then (12) has only one positive root, which is denoted by z_k. Hence, (11) has only one positive root $\omega_k = \sqrt{z_k}$. It follows from (10) that (8) with $k \in \mathbb{N}_0$ has a pair of purely imaginary roots $\pm i\omega_k$ when $\tau = \tau_k^j$, $j = 0, 1, 2, \ldots$, where

$$\omega_k = \left[\frac{-\left(A_k^2 - 2B_k\right) + \sqrt{\left(A_k^2 - 2B_k\right)^2 - 4\left(B_k^2 - C^2\right)}}{2}\right]^{\frac{1}{2}}, \tag{13}$$

$$\tau_k^j = \frac{1}{\omega_k}\left[\arccos\frac{\omega_k^2 - B_k}{C} + 2j\pi\right], \ j = 0, 1, 2, \ldots . \tag{14}$$

Lemma 1. *Assume that (3) and* $d_1 d_2\left(\frac{k}{l}\right)^4 - \left(d_1\beta_2 + d_2\alpha_1\right)\left(\frac{k}{l}\right)^2 + \alpha_1\beta_2 + \alpha_2(\beta_3 - \beta_1) < 0$ *hold; then,*

$$\left.\frac{d\Delta_k\left(\lambda, \tau_k^j\right)}{d\lambda}\right|_{\lambda = i\omega_k} \neq 0.$$

Therefore, $\lambda = i\omega_k$ *is a simple root of (8) for* $k \in \mathbb{N}_0$.

Proof. It follows from (9) that

$$\left.\frac{d\Delta_k\left(\lambda, \tau_k^j\right)}{d\lambda}\right|_{\lambda = i\omega_k} = 2\omega_k i + A_k - \tau_k^j C e^{-i\omega_k\tau_k^j}.$$

Differentiating both sides of $\Delta_k(\lambda, \tau) = 0$ with respect to τ yields

$$\left[2\lambda + A_k - \tau C e^{-\lambda\tau}\right]\frac{d\lambda(\tau)}{d\tau} = \lambda C e^{-\lambda\tau}.$$

If $\left.\frac{d\Delta_k\left(\lambda, \tau_k^j\right)}{d\lambda}\right|_{\lambda = i\omega_k} = 0$, then

$$i\omega_k C e^{-i\omega_k\tau_k^j} = 0.$$

Since $\omega_k > 0$ and $C > 0$, we have

$$i\omega_k C e^{-i\omega_k\tau_k^j} \neq 0,$$

which leads to a contradiction. Hence,

$$\left.\frac{d\Delta_k\left(\lambda, \tau_k^j\right)}{d\lambda}\right|_{\lambda = i\omega_k} \neq 0.$$

□

Lemma 2. *Assume that (3) and* $d_1d_2\left(\frac{k}{l}\right)^4-(d_1\beta_2+d_2\alpha_1)\left(\frac{k}{l}\right)^2+\alpha_1\beta_2+\alpha_2(\beta_3-\beta_1)<0$ *hold. Let* $\lambda(\tau)=\sigma(\tau)+i\omega(\tau)$ *be the root of Equation (8) satisfying* $\sigma\left(\tau_k^j\right)=0, \omega\left(\tau_k^j\right)=\omega_k$. *Then,* $\lambda(\tau)$ *satisfies the following transversality condition:*

$$sign\left\{Re\left(\frac{d\lambda}{d\tau}\right)\right\}_{\tau=\tau_k^j}>0.$$

Proof. Differentiating both sides of Equation (32) with respect to τ, we obtain

$$\left(\frac{d\lambda}{d\tau}\right)^{-1}=\frac{2e^{\lambda\tau}}{C}+\frac{A_ke^{\lambda\tau}}{C\lambda}-\frac{\tau}{\lambda}.$$

From (10), we can easily obtain

$$\begin{aligned}&sign\left[\mathrm{Re}\left(\frac{d\lambda}{d\tau}\right)^{-1}\right]_{\tau=\tau_k^j}\\&=sign\mathrm{Re}\left[\frac{2e^{\lambda\tau}}{C}+\frac{A_ke^{\lambda\tau}}{C\lambda}-\frac{\tau}{\lambda}\right]_{\tau=\tau_k^j}\\&=sign\left[\frac{2\cos\left(\omega_k\tau_k^j\right)}{C}+\frac{A_k\sin\left(\omega_k\tau_k^j\right)}{C\omega_k}\right].\end{aligned}$$

It is easy to show from (10) and the expression of ω_k that

$$sign\left[\mathrm{Re}\left(\frac{d\lambda}{d\tau}\right)^{-1}\right]_{\tau=\tau_k^j}=sign\left[\frac{\sqrt{\left(A_k^2-2B_k\right)^2-4\left(B_k^2-C^2\right)}}{C^2}\right]_{\tau=\tau_k^j}>0.$$

Then, we can verify the conclusion. □

Notice that Equation (8) with $k=0$ is the characteristic equation of the linearization of (2) without diffusion at the positive constant steady state. By Rouché theorem, we have the following result.[36,37]

Theorem 1. *Assume that (3) holds. The following statements hold:*

(i) If $\tau\in[0,\tau_0^0)$, *then all roots of Equation (8) with* $k=0$ *have negative real parts;*
(ii) If $\tau>\tau_0^0$, *then Equation (8) with* $k=0$ *has at least one root with positive real part;*
(iii) If $\tau=\tau_0^0$, *then Equation (8) with* $k=0$ *has a pair of simple purely imaginary roots* $\pm i\omega_0$, *and all roots of (8) with* $k=0$, *except* $\pm i\omega_0$, *have negative real parts.*

Furthermore, we can acquire the following results:

Theorem 2. *Assume that (3) holds. Then equation (8) with* $\tau=\tau_0^j$ $(j=0,1,2,\dots)$ *has a pair of simple purely imaginary roots* $\pm i\omega_0$, *and all roots of (8) for any* $k\in\mathbb{N}_0$, *except* $\pm i\omega_0$, *have no zero real parts. Moreover, for* $\tau=\tau_0^0$, *all roots of (8) for any* $k\in\mathbb{N}_0$, *except* $\pm i\omega_0$, *have negative real parts.*

Theorem 3. *Assume that (3) holds. The following statements hold:*

(i) If $\tau\in[0,\tau_0^0)$, *then the positive constant steady state* (u^*,v^*) *is asymptotically stable;*
(ii) If $\tau>\tau_0^0$, *then the positive constant steady state* (u^*,v^*) *is unstable;*
(iii) System (2) undergoes spatially homogeneous Hopf bifurcations near the positive constant steady state (u^*,v^*) *when* $\tau=\tau_0^j$ $(j=0,1,2,\dots)$.

τ_0^0	$<$	τ_0^1	$<$	τ_0^2	$<$	$\cdots$	$<$	τ_0^j	$<$ $\cdots$
$\wedge$		$\wedge$		$\wedge$		$\cdots$		$\wedge$	
τ_1^0	$<$	τ_1^1	$<$	τ_1^2	$<$	$\cdots$	$<$	τ_1^j	$<$ $\cdots$
$\wedge$		$\wedge$		$\wedge$		$\cdots$		$\wedge$	$\cdots$
$\vdots$		$\vdots$		$\vdots$		$\cdots$		$\vdots$	$\cdots$
$\wedge$		$\wedge$		$\wedge$		$\cdots$		$\wedge$	$\cdots$
τ_k^0	$<$	τ_k^1	$<$	τ_k^2	$<$	$\cdots$	$<$	τ_k^j	$<$ $\cdots$
$\wedge$		$\wedge$		$\wedge$		$\cdots$		$\wedge$	$\cdots$
$\vdots$		$\vdots$		$\vdots$		$\cdots$		$\vdots$	$\cdots$
$\wedge$		$\wedge$		$\wedge$		$\cdots$		$\wedge$	$\cdots$
$\tau_{K_0}^0$	$<$	$\tau_{K_0}^1$	$<$	$\tau_{K_0}^2$	$<$	$\cdots$	$<$	$\tau_{K_0}^j$	$<$ $\cdots$

TABLE 1 The sequence of τ_k^j for $0 \le k \le K_0$ and $j \in \mathbb{N}_0$

Denote

$$\widetilde{K} = \left[l^2 \frac{d_1\beta_2 + d_2\alpha_1 + \sqrt{(d_1\beta_2 + d_2\alpha_1)^2 - 4d_1d_2\,(\alpha_1\beta_2 + \alpha_2(\beta_3 - \beta_1))}}{2d_1d_2} \right]^{\frac{1}{2}},$$

$$K_0 = \begin{cases} \widetilde{K} - 1, \ \widetilde{K} \in \mathbb{N}, \\ \left[\widetilde{K}\right], \ \widetilde{K} \notin \mathbb{N}. \end{cases}$$

From Equation (14), we have $\tau_k^j < \tau_k^{j+1}$ for fixed $k \in [0, K_0]$ and any $j \in \mathbb{N}_0$. Sorting τ_k^j for fixed j, we have the following result.

Lemma 3. *Let τ_k^j be defined as Equation (14). Assume that (3) and $\frac{d_1d_2}{l^4} - \frac{d_1\beta_2 + d_2\alpha_1}{l^2} > 2\,(\alpha_2\beta_1 - \alpha_1\beta_2)$ hold. Then, for any $0 \le k \le K_0 - 1$, $j \in \mathbb{N}_0$, $\tau_k^j < \tau_{k+1}^j$.*

Proof. From (13), we have

$$\omega_k^2 = \frac{2}{\sqrt{\frac{\left(A_k^2 - 2B_k\right)^2}{\left(C^2 - B_k^2\right)^2} + \frac{4}{C^2 - B_k^2}} + \frac{A_k^2 - 2B_k}{C^2 - B_k^2}}.$$

By simple calculation, we can obtain that

$$\frac{d\left(A_k^2 - 2B_k\right)}{dk} = \frac{4\left(d_1^2 + d_2^2\right)}{l^4}k^3 - \frac{4\left(d_1\alpha_1 + d_2\beta_2\right)}{l^2}k,$$

$$\frac{d\left(C^2 - B_k^2\right)}{dk} = -2\left[\frac{d_1d_2k^4}{l^4} - \frac{(d_1\beta_2 + d_2\alpha_1)\,k^2}{l^2} + \alpha_1\beta_2 - \alpha_2\beta_1\right] \left[\frac{4d_1d_2k^3}{l^4} - \frac{2\,(d_1\beta_2 + d_2\alpha_1)\,k}{l^2}\right].$$

Obviously, $A_k^2 - 2B_k$ is strictly increasing in k for $1 \le k \le K_0$, and $A_1^2 - 2B_1 > A_0^2 - 2B_0$. $\frac{d_1d_2}{l^4} - \frac{d_1\beta_2 + d_2\alpha_1}{l^2} > 2\,(\alpha_2\beta_1 - \alpha_1\beta_2)$ guarantees that $C^2 - B_k^2$ is strictly decreasing in k for $1 \le k \le K_0$ and $C^2 - B_1^2 < C^2 - B_0^2$. Then, we obtain that ω_k is strictly decreasing in k for $0 \le k \le K_0$. Since B_k is strictly increasing in k for $0 \le k \le K_0$, then $\frac{\omega_k^2 - B_k}{C}$ is strictly decreasing in k for $0 \le k \le K_0$. So, $\arccos\frac{\omega_k^2 - B_k}{C}$ is strictly increasing in k for $0 \le k \le K_0$. Then, τ_k^j is strictly increasing in k for $0 \le k \le K_0$. □

Therefore, we have the following arrangement of τ_k^j for $0 \le k \le K_0$ and $j \in \mathbb{N}_0$ (see Table 1).

Denote

$$\Sigma := \left\{ \tau_k^j : \tau_k^j \ne \tau_{\widetilde{k}}^{j_1}, \ 0 \le \widetilde{k} < k \le K_0, \ j < j_1 \text{ or } 1 \le k < \widetilde{k} \le K_0, \ j > j_1, \ j, \ j_1 \in \mathbb{N}_0 \right\}.$$

From the above analysis, we have the following conclusion.

Theorem 4. *Assume that (3) and $d_1d_2\left(\frac{k}{l}\right)^4 - (d_1\beta_2 + d_2\alpha_1)\left(\frac{k}{l}\right)^2 + \alpha_1\beta_2 + \alpha_2(\beta_3 - \beta_1) < 0$ and $\frac{d_1d_2}{l^4} - \frac{d_1\beta_2 + d_2\alpha_1}{l^2} > 2\,(\alpha_2\beta_1 - \alpha_1\beta_2)$ hold. The following statements are true:*

(i) The positive constant steady state (u^*, v^*) is asymptotically stable for $\tau \in [0, \tau_0^0)$, and unstable when $\tau > \tau_0^0$.

(ii) System (2) undergoes inhomogeneous Hopf bifurcations near the positive constant steady state (u^*, v^*) when $\tau \in \Sigma$, ie, a family of spatially inhomogeneous periodic solutions bifurcating from (u^*, v^*) when τ crosses through the critical values $\tau \in \Sigma$.

3 | PROPERTIES OF HOPF BIFURCATIONS

In this section, we consider the direction, stability, and the period of bifurcating periodic solution by using the normal form theory and center manifold reduction for PFDEs developed by Wu.[14] Without loss of generality, denote any one of the critical values $\left\{\tau_0^j,\ j \in \mathbb{N}_0\right\} \cup \Sigma$ by τ^* at which (8) has simple pure imaginary roots $\pm i\omega_0 \cup \pm i\omega_k$, denoted by $\pm i\omega$. Normalizing the delay τ by the time-scaling $t \to t/\tau$, system (6) can be transformed into

$$\begin{cases} \frac{\partial u}{\partial t} = \tau \left[d_1 \Delta u + \alpha_1 u + \alpha_2 v + \sum\limits_{i+j\geq 2} \frac{1}{i!j!} f_{ij}^{(1)} u^j v^j \right], \\ \frac{\partial v}{\partial t} = \tau \left[d_2 \Delta v + \beta_1 u + \beta_2 v + \beta_3 u\left(x, t-1\right) + \sum\limits_{i+j+p\geq 2} \frac{1}{i!j!p!} f_{ijp}^{(2)} u^j\left(x,t\right) v^j\left(x,t\right) u^p\left(x,t-1\right) \right]. \end{cases} \tag{15}$$

Set $\mu = \tau - \tau^*$; then, $\mu = 0$ is a Hopf bifurcation value of system (2). Then, (15) can be rewritten in the fixed-phase space $\mathcal{C} = C\left([-1, 0], X\right)$ as

$$\frac{d}{dt} U(t) = \tau^* D \Delta U(t) + L(\tau^*)(U_t) + F(U_t, \mu), \tag{16}$$

where

$$L(\mu)\left(\varphi\right) = \mu \begin{pmatrix} \alpha_1 \varphi_1(0) + \alpha_2 \varphi_2(0) \\ \beta_1 \varphi_1(0) + \beta_2 \varphi_2(0) + \beta_3 \varphi_1(-1) \end{pmatrix},$$

$$F(\varphi, \mu) = \mu D \Delta \varphi(0) + L(\mu)\varphi + f(\varphi, \mu),$$

with

$$f(\varphi, \mu) = (\tau^* + \mu) \begin{pmatrix} \sum\limits_{i+j\geq 2} \frac{1}{i!j!} f_{ij}^{(1)} \varphi_1^i(0) \varphi_2^j(0) \\ \sum\limits_{i+j+p\geq 2} \frac{1}{i!j!p!} f_{ijp}^{(2)} \varphi_1^i(0) \varphi_2^j(0) \varphi_1^p(-1) \end{pmatrix}. \tag{17}$$

According to the Riesz representation theorem, there exists a 2×2 matrix function $\eta(\theta, \tau^*)$ $(-1 \leq \theta \leq 0)$, whose elements are of bounded variation such that

$$-\tau^* D \left(\frac{k}{l}\right)^2 \phi\left(0\right) + L(\tau^*)(\phi) = \int_{-1}^{0} d\left[\eta(\theta, \tau^*)\right] \phi(\theta) \text{ for } \phi \in C([-1, 0], \mathbb{R}^2).$$

We then define

$$\eta(\theta, \tau^*) = \begin{cases} \tau^* \begin{pmatrix} \alpha_1 - d_1\left(\frac{k}{l}\right)^2 & \alpha_2 \\ \beta_1 & \beta_2 - d_2\left(\frac{k}{l}\right)^2 \end{pmatrix}, & \theta = 0, \\ 0, & \theta \in (-1, 0), \\ -\tau^* \begin{pmatrix} 0 & 0 \\ \beta_3 & 0 \end{pmatrix}, & \theta = -1. \end{cases}$$

For $\phi \in C([-1, 0], \mathbb{R}^2)$, $\psi \in C([0, 1], \mathbb{R}^2)$, define A and A^* as

$$A\left(\phi\left(\theta\right)\right) = \begin{cases} \frac{d\phi(\theta)}{d\theta}, & \theta \in [-1, 0), \\ \int_{-1}^{0} d\left[\eta(\theta, \tau^*)\right] \phi(\theta), & \theta = 0, \end{cases}$$

$$A^*\left(\psi\left(\gamma\right)\right) = \begin{cases} -\frac{d\psi(\gamma)}{d\gamma}, & \gamma \in (0, 1], \\ \int_{-1}^{0} d\left[\eta(\theta, \tau^*)\right] \psi\left(-\theta\right), & \gamma = 0. \end{cases}$$

Then, A^* is the formal adjoint of A under the bilinear pairing

$$(\psi,\phi)=\overline{\psi}(0)\phi(0)+\tau^*\int_{-1}^{0}\overline{\psi}(\xi+1)\begin{pmatrix}0&0\\ \beta_3&0\end{pmatrix}\phi(\xi)d\xi. \tag{18}$$

It can be verified that $p(\theta)=e^{i\omega\tau^*\theta}(1,\xi)^T$, $\theta\in[-1,0]$ is an eigenvector of A corresponding to $i\omega\tau^*$, and $p^*(\gamma)=r(1,\eta)\,e^{i\omega\tau^*\gamma}$, $\gamma\in[0,1]$, is an eigenvector of A^* corresponding to $-i\omega\tau^*$, where

$$\xi=\frac{i\omega-\alpha_1+d_1\left(\frac{k}{l}\right)^2}{\alpha_2},\ \eta=\frac{-i\omega-\alpha_1+d_1\left(\frac{k}{l}\right)^2}{\beta_1+\beta_3e^{-i\omega\tau^*}},$$
$$\overline{r}=\left[1+\left(\xi+\tau^*\beta_3e^{-i\omega\tau^*}\right)\overline{\eta}\right]^{-1}.$$

Then, $P=\text{span}\left\{p(\theta),\overline{p}(\theta)\right\}$ and $P^*=\text{span}\left\{p^*(\gamma),\overline{p^*}(\gamma)\right\}$ are the center subspace.

Denote $f_k:=\left(\beta_k^1,\beta_k^2\right)$. Let $c\cdot f_k$ be defined by $c\cdot f_k=c_1\beta_k^1+c_2\beta_k^2$ for $c=(c_1,c_2)^T\in C([-1,0],X)$. Let $\langle\cdot,\cdot\rangle$ be the complex-valued L^2 inner product on Hilbert space X_C, defined as

$$\langle U_1,U_2\rangle=\frac{1}{l\pi}\int_0^{l\pi}u_1\bar{v}_1dx+\frac{1}{l\pi}\int_0^{l\pi}u_2\bar{v}_2dx \tag{19}$$

for $U_1=(u_1,u_2)^T$, $U_2=(v_1,v_2)^T\in X_C$. And $\left\langle\beta_0^1,\beta_0^1\right\rangle=1$, $\left\langle\beta_k^1,\beta_k^1\right\rangle=\frac{1}{2}$,$k\in\mathbb{N}$,

$$\langle\phi,f_k\rangle=\left(\left\langle\phi,\beta_k^1\right\rangle,\left\langle\phi,\beta_k^2\right\rangle\right)^T,\ \text{where }\phi\in C([-1,0],X). \tag{20}$$

Then, the center subspace of linear Equation (16) is given by $P_{CN}C$, where

$$P_{CN}C(\varphi)=\Phi(\Psi,\langle\varphi,f_k\rangle)\cdot f_k,\ \varphi\in C, \tag{21}$$

and $C=P_{CN}C\oplus Q$; here, Q denotes the complementary subspace of $P_{CN}C$. Following the algorithms in Hassard et al,[38] the solutions of (16) at $\mu=0$ are given by

$$U_t=\left(p(\theta)z(t)+\overline{p}(\theta)\overline{z}(t)\right)\cdot f_k+w\left(z(t),\overline{z}(t),\theta\right), \tag{22}$$

where

$$w\left(z,\overline{z}\right):=w\left(z(t),\overline{z}(t),\theta\right)=w_{20}(\theta)\frac{z^2}{2}+w_{11}(\theta)z\overline{z}+w_{02}(\theta)\frac{\overline{z}^2}{2}+\ \dots\ . \tag{23}$$

From,[14] z satisfies

$$\dot{z}=i\omega\tau^*z+g(z,\overline{z}), \tag{24}$$

where

$$g(z,\overline{z})=\overline{p^*}(0)\langle f(U_t,0),f_k\rangle=g_{20}\frac{z^2}{2}+g_{11}z\overline{z}+g_{02}\frac{\overline{z}^2}{2}+g_{21}\frac{z^2\overline{z}}{2}+\ \dots\ . \tag{25}$$

Notice that $\int_0^{l\pi}\cos^3\frac{kx}{l}dx=0$, $\frac{1}{l\pi}\int_0^{l\pi}\cos^3\frac{kx}{l}dx=\frac{3}{8}$, $k\in\mathbb{N}$ and combining (17) to (24), we obtain the following equations:

$$g_{20}=\begin{cases}0,\ k=1,2,\ \dots\ ,K_0,\\ \bar{r}\tau^*\left\{f_{20}^{(1)}+f_{02}^{(1)}\xi^2+2f_{11}^{(1)}\xi+\bar{\eta}\left[f_{200}^{(2)}+f_{020}^{(2)}\xi^2\right.\right.\\ \left.\left.+2\left(f_{110}^{(2)}\xi+f_{101}^{(2)}e^{-i\omega\tau^*}+f_{011}^{(2)}\xi e^{-i\omega\tau^*}\right)\right]\right\},\ k=0,\end{cases}$$

$$g_{02}=\overline{g_{20}},$$

$$g_{11}=\begin{cases}0,\ k=1,2,\ \dots\ ,K_0,\\ \bar{r}\tau^*\left\{f_{20}^{(1)}+f_{02}^{(1)}\xi\bar{\xi}+2f_{11}^{(1)}\mathrm{Re}(\xi)+\bar{\eta}\left[f_{200}^{(2)}+f_{020}^{(2)}\xi\bar{\xi}+2f_{110}^{(2)}\mathrm{Re}(\xi)\right.\right.\\ \left.\left.+f_{101}^{(2)}\left(e^{i\omega\tau^*}+e^{-i\omega\tau^*}\right)+f_{011}^{(2)}\left(\xi e^{i\omega\tau^*}+\bar{\xi}e^{-i\omega\tau^*}\right)\right]\right\},\ k=0,\end{cases}$$

$$\begin{aligned}g_{21}=\frac{\bar{r}\tau^*}{l\pi}\Bigg\{&\int_0^{l\pi}\left[f_{20}^{(1)}\left(2w_{11}^1(0)+w_{20}^1(0)\right)+f_{02}^{(1)}\left(2\xi w_{11}^2(0)+\bar{\xi}w_{20}^2(0)\right)\right]\cos^2\frac{kx}{l}dx\\ &+\int_0^{l\pi}\left[f_{11}^{(1)}\left(2w_{11}^2(0)+w_{20}^2(0)+\bar{\xi}w_{20}^1(0)+2\xi w_{11}^1(0)\right)\right]\cos^2\frac{kx}{l}dx\\ &+\left[f_{30}^{(1)}+f_{03}^{(1)}\xi^2\bar{\xi}+f_{12}^{(1)}\left(\xi^2+2|\xi|^2\right)+f_{21}^{(1)}\left(2\xi+\bar{\xi}\right)\right]\int_0^{l\pi}\cos^4\frac{kx}{l}dx\\ &+\bar{\eta}\Bigg[\int_0^{l\pi}\left[f_{200}^{(2)}\left(2w_{11}^1(0)+w_{20}^1(0)\right)+f_{020}^{(2)}\left(2\xi w_{11}^2(0)+\bar{\xi}w_{20}^2(0)\right)\right.\\ &+f_{110}^{(2)}\left(2w_{11}^2(0)+w_{20}^2(0)+\bar{\xi}w_{20}^1(0)+2\xi w_{11}^1(0)\right)\\ &+f_{101}^{(2)}\left(2e^{-i\omega\tau^*}w_{11}^2(0)+e^{i\omega\tau^*}w_{20}^1(0)+w_{20}^1(-1)+2w_{11}^1(-1)\right)\\ &\left.+f_{011}^{(2)}\left(2e^{-i\omega\tau^*}w_{11}^2(0)+e^{i\omega\tau^*}w_{20}^2(0)+\bar{\xi}w_{20}^1(-1)+2\xi w_{11}^1(-1)\right)\right]\cos^2\frac{kx}{l}dx\\ &+\left[f_{300}^{(2)}+f_{030}^{(2)}\xi^2\bar{\xi}+f_{120}^{(2)}\left(\xi^2+2|\xi|^2\right)+f_{210}^{(2)}\left(\bar{\xi}+2\xi\right)\right.\\ &+f_{021}^{(2)}\left(\xi^2e^{i\omega\tau^*}+2\xi\bar{\xi}e^{-i\omega\tau^*}\right)+f_{201}^{(2)}\left(e^{i\omega\tau^*}+2e^{-i\omega\tau^*}\right)\\ &\left.+\ f_{111}^{(2)}\left(\xi e^{i\omega\tau^*}+2\mathrm{Re}(\xi)e^{-i\omega\tau^*}\right)\right]\int_0^{l\pi}\cos^4\frac{kx}{l}dx\Bigg]\Bigg\},\ k=0,1,2,\ \dots\ ,K_0.\end{aligned}$$

Since $w_{20}(\theta)$ and $w_{11}(\theta)$ are included in g_{21}, we still need to compute them. By Wu,[14] $w(z,\bar{z})$ satisfies

$$\dot{w}=Aw+H(z,\bar{z}),\tag{26}$$

where

$$\begin{aligned}Aw&=Aw_{20}(\theta)\frac{z^2}{2}+Aw_{11}(\theta)z\bar{z}+Aw_{02}(\theta)\frac{\bar{z}^2}{2}+\ \dots\ .\\ H(z,\bar{z})&=H_{20}\frac{z^2}{2}+H_{11}z\bar{z}+H_{02}\frac{\bar{z}^2}{2}+\ \dots\\ &=X_0f(U_t,0)-\Phi(\Psi,\langle X_0f(U_t,0),f_k\rangle)\cdot f_k,\end{aligned}\tag{27}$$

with

$$X_0(\theta)=\begin{cases}0,\ \theta\in[-1,0),\\ I,\ \theta=0.\end{cases}$$

According to (23), (24), (26), and (27), we have

$$w_{20}=(2i\omega\tau^*-A)^{-1}H_{20},\ w_{11}=-A^{-1}H_{11}.\tag{28}$$

From (27), we know that for $\theta \in [-1, 0)$,

$$H(z,\bar{z}) = -\left(p(\theta)g_{20} + \bar{p}(\theta)\bar{g}_{02}\right)\cos\frac{kx}{l}\frac{z^2}{2} - \left(p(\theta)g_{11} + \bar{p}(\theta)\bar{g}_{11}\right)\cos\frac{kx}{l}z\bar{z} + \ \dots \ .$$

Therefore, for $\theta \in [-1, 0)$,

$$H_{20}(\theta) = \begin{cases} 0, & k \in \mathbb{N}, \\ -g_{20}p(\theta) - \bar{g}_{02}\bar{p}(\theta), & k = 0, \end{cases}$$

$$H_{11}(\theta) = \begin{cases} 0, & k \in \mathbb{N}, \\ -g_{11}p(\theta) - \bar{g}_{11}\bar{p}(\theta), & k = 0, \end{cases}$$

and

$$H(z,\bar{z})(0) = f(U_t, 0) - \Phi(\Psi, \langle f(U_t, 0), f_k\rangle \cdot f_k).$$

Hence, for $\theta = 0$, we have

$$H_{20}(0) = \begin{cases} \tau^* \begin{pmatrix} f_{20}^{(1)} + f_{02}^{(1)}\xi^2 + 2f_{11}^{(1)}\xi + f_{200}^{(2)} + f_{020}^{(2)}\xi^2 \\ +2\left(f_{110}^{(2)}\xi + f_{101}^{(2)}e^{-i\omega\tau^*} + f_{011}^{(2)}\xi e^{-i\omega\tau^*}\right) \end{pmatrix}\cos^2\frac{kx}{l}, \\ k = 1, 2, \ \dots \ , K_0, \\ \tau^* \begin{pmatrix} f_{20}^{(1)} + f_{02}^{(1)}\xi^2 + 2f_{11}^{(1)}\xi + f_{200}^{(2)} + f_{020}^{(2)}\xi^2 \\ +2\left(f_{110}^{(2)}\xi + f_{101}^{(2)}e^{-i\omega\tau^*} + f_{011}^{(2)}\xi e^{-i\omega\tau^*}\right) \end{pmatrix} \\ -g_{20}p(0) - \bar{g}_{02}\bar{p}(0), \ k = 0. \end{cases}$$

$$H_{11}(0) = \begin{cases} \tau^* \begin{pmatrix} f_{20}^{(1)} + f_{02}^{(1)}\xi\bar{\xi} + 2f_{11}^{(1)}\mathrm{Re}(\xi) + f_{200}^{(2)} + f_{020}^{(2)}\xi\bar{\xi} + 2f_{110}^{(2)}\mathrm{Re}(\xi) \\ +f_{101}^{(2)}\left(e^{i\omega\tau^*} + e^{-i\omega\tau^*}\right) + f_{011}^{(2)}\left(\xi e^{i\omega\tau^*} + \bar{\xi}e^{-i\omega\tau^*}\right) \end{pmatrix}\cos^2\frac{kx}{l}, \\ k = 1, 2, \ \dots \ , K_0, \\ \tau^* \begin{pmatrix} f_{20}^{(1)} + f_{02}^{(1)}\xi\bar{\xi} + 2f_{11}^{(1)}\mathrm{Re}(\xi) + f_{200}^{(2)} + f_{020}^{(2)}\xi\bar{\xi} + 2f_{110}^{(2)}\mathrm{Re}(\xi) \\ +f_{101}^{(2)}\left(e^{i\omega\tau^*} + e^{-i\omega\tau^*}\right) + f_{011}^{(2)}\left(\xi e^{i\omega\tau^*} + \bar{\xi}e^{-i\omega\tau^*}\right) \end{pmatrix} \\ -g_{11}p(0) - \bar{g}_{11}\bar{p}(0), \ k = 0. \end{cases}$$

By the definition of A and $p(\theta) = p(0)e^{i\omega\tau^*\theta}$ $\theta \in [-1, 0]$, we can obtain

$$\begin{cases} w_{20}(\theta) = i\left[\frac{p(\theta)g_{20}}{\omega\tau^*} + \frac{\bar{p}(\theta)\bar{g}_{02}}{3\omega\tau^*}\right]\cdot f_k + e^{2i\omega\tau^*\theta}E_1, \\ w_{11}(\theta) = \frac{i}{\omega\tau^*}\left(\bar{p}(\theta)\bar{g}_{11} - p(\theta)g_{11}\right) + E_2. \end{cases} \tag{29}$$

Using the definition of A and combining (28) and (29), we obtain

$$E_1 = \widetilde{E}_1 \begin{pmatrix} f_{20}^{(1)} + f_{02}^{(1)}\xi^2 + 2f_{11}^{(1)}\xi + f_{200}^{(2)} + f_{020}^{(2)}\xi^2 \\ +2\left(f_{110}^{(2)}\xi + f_{101}^{(2)}e^{-i\omega\tau^*} + f_{011}^{(2)}\xi e^{-i\omega\tau^*}\right) \end{pmatrix}\cos^2\frac{kx}{l},$$

$$E_2 = \widetilde{E}_2 \begin{pmatrix} f_{20}^{(1)} + f_{02}^{(1)}\xi\bar{\xi} + 2f_{11}^{(1)}\mathrm{Re}(\xi) + f_{200}^{(2)} + f_{020}^{(2)}\xi\bar{\xi} + 2f_{110}^{(2)}\mathrm{Re}(\xi) \\ +f_{101}^{(2)}\left(e^{i\omega\tau^*} + e^{-i\omega\tau^*}\right) + f_{011}^{(2)}\left(\xi e^{i\omega\tau^*} + \bar{\xi}e^{-i\omega\tau^*}\right) \end{pmatrix}\cos^2\frac{kx}{l},$$

where

$$\widetilde{E}_1 = \begin{pmatrix} 2i\omega + d_1\left(\frac{k}{l}\right)^2 - \alpha_1 & -\alpha_2 \\ -\beta_1 - \beta_3 e^{-2i\omega\tau^*} & 2i\omega + d_2\left(\frac{k}{l}\right)^2 - \beta_2 \end{pmatrix}^{-1},$$

$$\widetilde{E}_2 = \begin{pmatrix} d_1\left(\frac{k}{l}\right)^2 - \alpha_1 & -\alpha_2 \\ -\beta_1 - \beta_3 & d_2\left(\frac{k}{l}\right)^2 - \beta_2 \end{pmatrix}^{-1}.$$

So far, g_{21} can be expressed by the parameter of system (3).

Thus, the properties of bifurcating periodic solutions at the critical value τ^* are determined by the sign of μ_2, σ_2, T_2, where

$$\begin{cases} c_1(\tau^*) = \frac{i}{2\omega\tau^*}\left(g_{11}g_{20} - 2|g_{11}|^2 - \frac{|g_{02}|^2}{3}\right) + \frac{g_{21}}{2}, \\ \mu_2 = -\frac{\mathrm{Re}\left(c_1(\tau^*)\right)}{\mathrm{Re}(\lambda'(\tau^*))}, \\ \sigma_2 = 2\mathrm{Re}\left(c_1(\tau^*)\right), \\ T_2 = -\frac{\mathrm{Im}\left(c_1(\tau^*)\right) + \mu_2 \mathrm{Im}(\lambda'(\tau^*))}{\omega\tau^*}. \end{cases}$$

According to the results in Hassard et al,[38] the properties of the Hopf bifurcation can be determined by μ_2: if $\mu_2 > 0$ ($\mu_2 < 0$), then the Hopf bifurcation is supercritical (subcritical) and the bifurcating periodic solutions exists for $\tau > \tau^*$ ($\tau < \tau^*$); σ_2 determines the stability of the bifurcating periodic solutions: the bifurcating periodic solutions on the center manifold are stable (unstable) if $\sigma_2 < 0$ ($\sigma_2 > 0$); the period increase (decrease) if $T_2 > 0$ ($T_2 < 0$).

4 | CROSS-FRACTIONAL DIFFUSION–INDUCED TURING INSTABILITY

In this section, we study the cross-fractional diffusion–driven instability of the positive constant steady state (u^*, v^*) in system (4). It is obvious that (u^*, v^*) is also the unique positive constant steady state of (4) if (3) holds. Fang and Wang[6] proved that the positive constant steady state (u^*, v^*) of system (2) with $\tau = 0$ is globally asymptotically stable, which implies self diffusion of system (2) with $\tau = 0$ does not trigger the Turing instability. However, we will show that the instability induced by the cross-fractional diffusion is possible.

The linearized system of (4) at (u^*, v^*) is

$$\frac{\partial \Phi}{\partial t} = D\nabla^\gamma \Phi + K(\Phi), \tag{30}$$

where

$$\Phi(x,t) = \begin{pmatrix} u(x,t) \\ v(x,t) \end{pmatrix}, \ D = \begin{pmatrix} d_1 & d_{12} \\ d_{21} & d_2 \end{pmatrix},$$

$$K = \begin{pmatrix} \alpha_1 & \alpha_2 \\ \widetilde{\beta}_1 & \beta_2 \end{pmatrix} = \begin{pmatrix} -\frac{be^2u^*}{(eu^*+cv^*)^2} & -u^*\left[\frac{bce}{(eu^*+cv^*)^2} + d\right] \\ dv^* - \frac{bcev^*}{(eu^*+cv^*)^2} & -\frac{bc^2v^*}{(eu^*+cv^*)^2} \end{pmatrix}.$$

For system (30), we pursue the general solution

$$\begin{pmatrix} u \\ v \end{pmatrix} = \begin{pmatrix} \mu_1 \\ \mu_2 \end{pmatrix} \exp(\lambda t + i\mathbf{k}\cdot x) \tag{31}$$

to the linearization of (4) as a superposition of normal modes. Here, λ is the growth rate of the perturbation in time t, i is the imaginary unit, and $\mathbf{k}$ is its wave vector. Substituting (31) into (30), we get the following matrix equation:

$$\begin{pmatrix} \lambda + d_1k^\gamma - \alpha_1 & d_{12}k^\gamma - \alpha_2 \\ d_{21}k^\gamma - \widetilde{\beta}_1 & \lambda + d_2k^\gamma - \beta_2 \end{pmatrix} \begin{pmatrix} \mu_1 \\ \mu_2 \end{pmatrix} = \begin{pmatrix} 0 \\ 0 \end{pmatrix},$$

where the Euclidean norm $k = |\mathbf{k}|$ is the wavenumber of the perturbation. Therefore, we obtain the following dispersion relation:

$$\lambda^2 + T(k)\lambda + D(k) = 0, \tag{32}$$

where

$$T(k) = (d_1 + d_2)k^\gamma - (\alpha_1 + \beta_2),$$

$$D(k) = (d_1d_2 - d_{12}d_{21})k^{2\gamma} + \left(d_{12}\widetilde{\beta}_1 + d_{21}\alpha_2 - d_1\beta_2 - d_2\alpha_1\right)k^\gamma + \alpha_1\beta_2 - \alpha_2\widetilde{\beta}_1.$$

Now, we will verify the instability of (u^*, v^*) caused by cross-fractional diffusion.

Theorem 5. *Suppose that (3), $d_{12} + d_{21} \neq 0$, and $d_1d_2 > d_{12}d_{21}$ hold. Then, there exists an unbounded domain Λ in $d_{12} - d_{21}$ plan defined by*

$$\Lambda = \left\{ (d_{12}, d_{21}) \in \mathbb{R}^2 | d_{12}\widetilde{\beta}_1 + d_{21}\alpha_2 < d_1\beta_2 + d_2\alpha_1 - 2\sqrt{\left(\alpha_1\beta_2 - \alpha_2\widetilde{\beta}_1\right)(d_1d_2 - d_{12}d_{21})} \right\}, \tag{33}$$

such that (u^*, v^*) *is unstable for the system (4) if* $(d_{12}, d_{21}) \in \Lambda$.

Proof. The eigenvalues $\lambda(k)$ of (32) are given by

$$\lambda(k) = \frac{-T(k) \pm \sqrt{T^2(k) - 4D(k)}}{2}.$$

Note that $T(0) = -(\alpha_1 + \beta_2) > 0$, hence $T(k) > 0$ for all $k \geq 0$. To achieve the instability of (u^*, v^*), it is necessary to ensure $D(k) < 0$ for some $k > 0$ since $D(0) = \alpha_1\beta_2 - \alpha_2\widetilde{\beta}_1 > 0$. Note that in the absence of cross-fractional diffusion (ie, $d_{12} = d_{21} = 0$), one has $D(k) > 0$, which implies that self fraction diffusion still cannot create Turing instability. $D(k)$ arrives at its minimum denoted by $\min\limits_{k\geq 0} D(k)$ when

$$k = k_{\min} = \left(\frac{d_1\beta_2 + d_2\alpha_1 - d_{12}\widetilde{\beta}_1 - d_{21}\alpha_2}{2\left(d_1d_2 - d_{12}d_{21}\right)}\right)^{\frac{1}{\gamma}} > 0,$$

and

$$\min_{k\geq 0} D(k) = \alpha_1\beta_2 - \alpha_2\widetilde{\beta}_1 - \frac{\left(d_1\beta_2 + d_2\alpha_1 - d_{12}\widetilde{\beta}_1 - d_{21}\alpha_2\right)^2}{2\left(d_1d_2 - d_{12}d_{21}\right)}.$$

$d_1d_2 > d_{12}d_{21}$ implies that (d_{12}, d_{21}) falls into the region between the two components of the hyperbola $d_1d_2 = d_{12}d_{21}$ in $d_{12} - d_{21}$ plan (see Figure 1, left).

Summarizing the above analysis, we get the instability domain of (u^*, v^*) in $d_{12} - d_{21}$ plan as follows:

$$\Lambda = \left\{(d_{12}, d_{21}) \in \mathbb{R}^2 | d_{12}\widetilde{\beta}_1 + d_{21}\alpha_2 < d_1\beta_2 + d_2\alpha_1 - 2\sqrt{\left(\alpha_1\beta_2 - \alpha_2\widetilde{\beta}_1\right)\left(d_1d_2 - d_{12}d_{21}\right)}\right\}.$$

□

Remark 1. In terms of the disperse relation (32), we illustrate in Figure 1 (right) the real part of the eigenvalue corresponding to three different sets of parameters as a function of the wavenumber; one can see that the wavenumber range of Turing instability increases with the decreases of order of fractional diffusion, which implies that the smaller order of fractional diffusion is, the more easily Turing instability is able to occur. In particular, if $\gamma = 2$, then (4) reduces to a cross diffusion system, and our result in Theorem 5 is still holds.

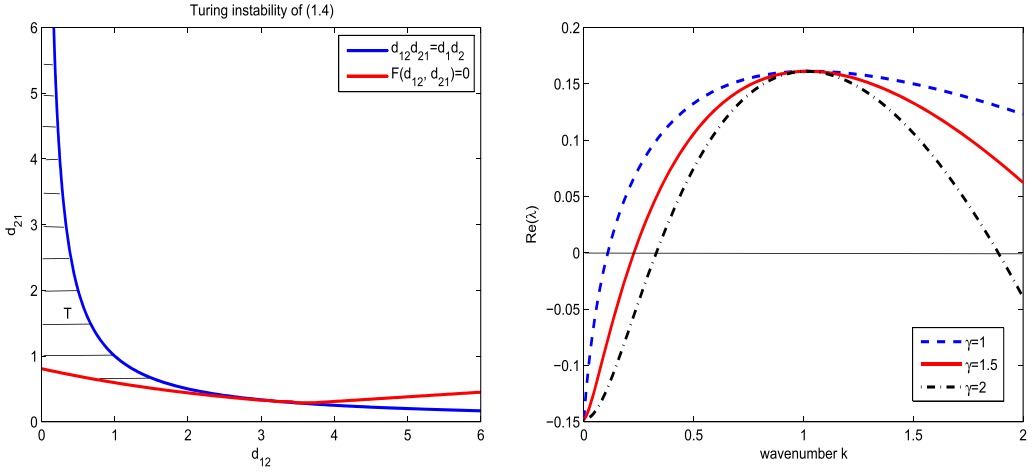

FIGURE 1 (Left): The parameters of (4) are $b = 1.5$, $c = 0.1$, $d = 0.25$, $e = 0.2$, $m = 0.1$, $n = 0.7$, $d_1 = d_2 = 1$. T is the Turing instability domain, where $F(d_{12}, d_{21}) = -(d_{12}\widetilde{\beta}_1 + d_{21}\alpha_2) + d_1\beta_2 + d_2\alpha_1 - 2\sqrt{(\alpha_1\beta_2 - \alpha_2\widetilde{\beta}_1)(d_1d_2 - d_{12}d_{21})}$. (Right): Let $d_{12} = 0.4$, $d_{21} = 2$, the dispersion relation of system (4) for three different $\gamma = 1, 1.5, 2$ [Colour figure can be viewed at wileyonlinelibrary.com]

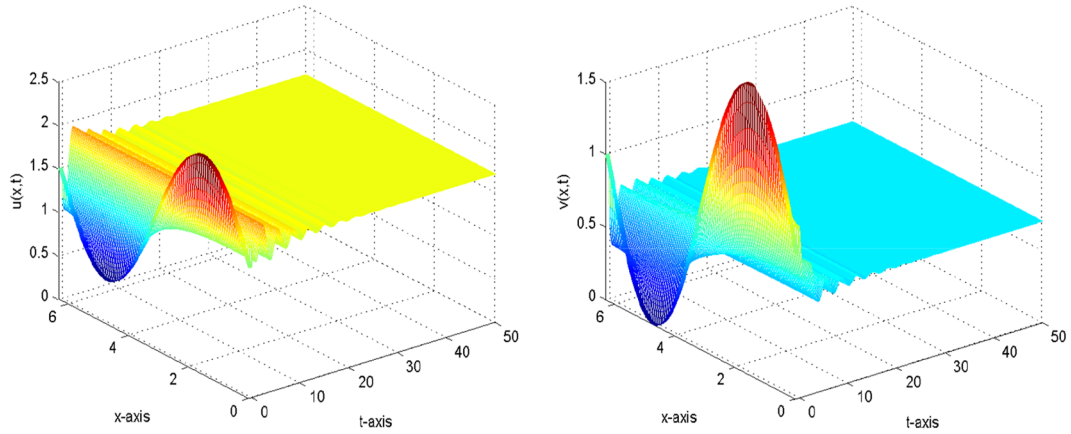

FIGURE 2 Numerical simulations of system (2) with the parameters given in Example 1, $\tau = 5.3$, and initial values $u(x,t) = 1.5\sin x$, $v(x,t) = \sin x$, $(x,t) \in [0, 2\pi] \times [-5.3, 0]$. The positive constant steady state $(1.6462, 0.7538)$ is asymptotically stable [Colour figure can be viewed at wileyonlinelibrary.com]

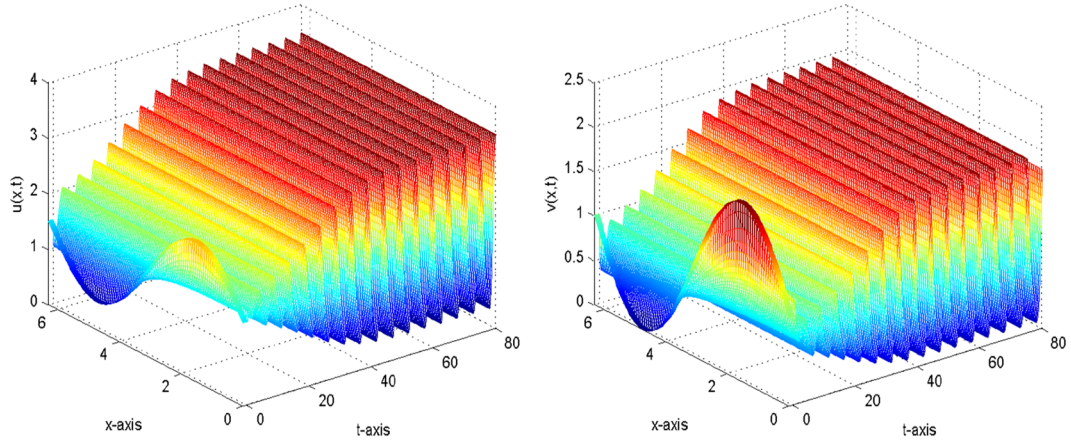

FIGURE 3 Numerical simulations of system (2) with the parameters given in Example 1, $\tau = 6.2$, and initial values $u(x,t) = 1.5\sin x$, $v(x,t) = \sin x$, $(x,t) \in [0, 2\pi] \times [-6.2, 0]$. The positive constant steady state $(1.6462, 0.7538)$ is unstable, and the bifurcating periodic solutions from $(1.6462, 0.7538)$ are stable [Colour figure can be viewed at wileyonlinelibrary.com]

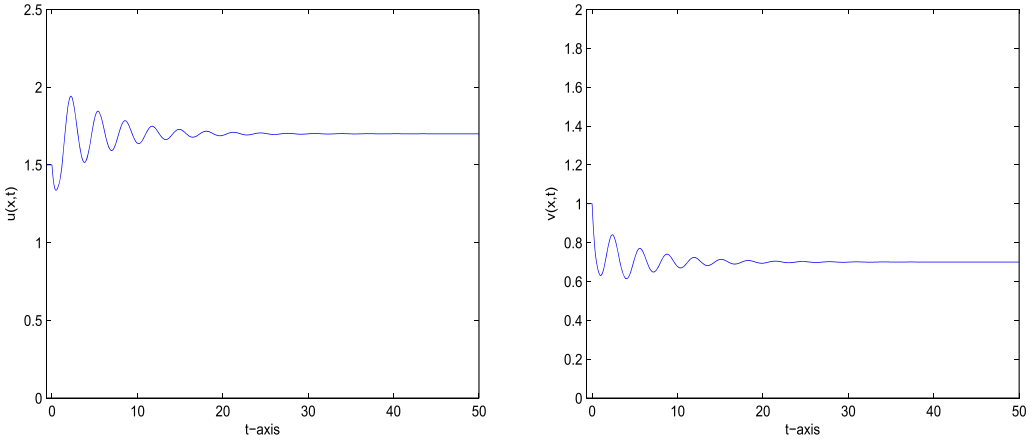

FIGURE 4 Numerical simulations of system (2) with the parameters given in Example 1 at mesh point $x_{100} = \pi$ plotted against $t_{\mathbf{n}} = \mathbf{n}\Delta t$ with $\tau = 5.2$ [Colour figure can be viewed at wileyonlinelibrary.com]

TABLE 2 Numerical solution $U_{100}^{\mathbf{n}}$ when $\mathbf{n} = 40\mathbf{k}$ ($\mathbf{k} = 1, 2, \ldots, 25$)

Solution	40	2 × 40	3 × 40	4 × 40	5 × 40	6 × 40	7 × 40
$U_{100}^{\mathbf{n}}$	1.8630	1.4736	1.6990	1.6799	1.5856	1.6884	1.6362
Solution	8 × 40	9 × 40	10 × 40	11 × 40	12 × 40	13 × 40	14 × 40
$U_{100}^{\mathbf{n}}$	1.6344	1.6627	1.6362	1.6475	1.6500	1.6419	1.6485
Solution	15 × 40	16 × 40	17 × 40	18 × 40	19 × 40	20 × 40	21 × 40
$U_{100}^{\mathbf{n}}$	1.6462	1.6451	1.6473	1.6457	1.6461	1.6462	1.6462
Solution	22 × 40	23 × 40	24 × 40	25 × 40			
$U_{100}^{\mathbf{n}}$	1.6462	1.6462	1.6462	1.6462			

TABLE 3 The numerical solution $V_{100}^{\mathbf{n}}$ when $\mathbf{n} = 40\mathbf{k}(\mathbf{k} = 1, 2, \ldots, 25)$

Solution	40	2 × 40	3 × 40	4 × 40	5 × 40	6 × 40	7 × 40
$V_{100}^{\mathbf{n}}$	0.8591	0.6680	0.8023	0.7514	0.7307	0.7772	0.7429
Solution	8 × 40	9 × 40	10 × 40	11 × 40	12 × 40	13 × 40	14 × 40
$V_{100}^{\mathbf{n}}$	0.7525	0.7606	0.7479	0.7561	0.7546	0.7519	0.7553
Solution	15 × 40	16 × 40	17 × 40	18 × 40	19 × 40	20 × 40	21 × 40
$V_{100}^{\mathbf{n}}$	0.7533	0.7535	0.7543	0.7534	0.7539	0.7539	0.7537
Solution	22 × 40	23 × 40	24 × 40	25 × 40			
$V_{100}^{\mathbf{n}}$	0.7538	0.7538	0.7538	0.7538			

TABLE 4 The numerical solution $U_{100}^{\mathbf{n}}$ when $\mathbf{n} = 10\mathbf{k}$ ($\mathbf{k} = 119, 120, \ldots, 160$)

Solution	1190	1200	1210	1220	1230	1240	1250
$U_{100}^{\mathbf{n}}$	3.1981	2.3766	1.4642	0.8358	0.4900	0.3445	0.4154
Solution	1260	1270	1280	1290	1300	1310	1320
$U_{100}^{\mathbf{n}}$	1.0158	2.3823	3.3014	3.3676	2.7561	1.8043	1.0488
Solution	1330	1340	1350	1360	1370	1380	1390
$U_{100}^{\mathbf{n}}$	0.5999	0.3812	0.3997	0.6743	1.7962	3.0525	3.4258
Solution	1400	1410	1420	1430	1440	1450	1460
$U_{100}^{\mathbf{n}}$	3.0778	2.1843	1.3140	0.7417	0.4464	0.3362	0.4729
Solution	1470	1480	1490	1500	1510	1520	1530
$U_{100}^{\mathbf{n}}$	1.2399	2.6398	3.3728	3.3010	2.5757	1.6320	0.9379
Solution	1540	1550	1560	1570	1580	1590	1600
$U_{100}^{\mathbf{n}}$	0.5414	0.3590	0.3728	0.8193	2.0863	3.1938	3.4122

5 | NUMERICAL SIMULATIONS

In this section, we present some numerical simulations and computations that complement the theoretical analysis in Section 3.

Example 1. In system (2), set $d_1 = 0.4$, $d_2 = 1$, $l = 2$, $b = 1.5$, $c = 0.1$, $d = 0.25$, $e = 0.2$, $m = 0.1$, $n = 0.7$. By computation, we have $(u^*, v^*) \approx (1.6462, 0.7538)$. Equation (13) has two positive roots $\omega_0 \approx 0.1584$, $\omega_1 \approx 0.1023$, and $\tau_0^0 \approx 5.7754 < \tau_1^0 \approx 19.9272$. $d_1 d_2 \left(\frac{1}{l}\right)^4 - (d_1\beta_2 + d_2\alpha_1)\left(\frac{1}{l}\right)^2 + \alpha_1\beta_2 + \alpha_2(\beta_3 - \beta_1) \approx -0.0633$ and $\frac{d_1 d_2}{l^4} - \frac{d_1\beta_2 + d_2\alpha_1}{l^2} - 2(\alpha_2\beta_1 - \alpha_1\beta_2) = 0.0143$. When the conditions of Theorem 4 are satisfied, then $(1.6462, 0.7538)$ is asymptotically stable when $0 < \tau < \tau_0^0 \approx 5.7754$ and unstable when $\tau > \tau_0^0 \approx 5.7754$, and when τ crosses increasingly through $\tau_0^0 \approx 5.7754$ and $\tau_1^0 \approx 19.9272$, a spatially homogeneous and inhomogeneous periodic solutions bifurcate from $(1.6462, 0.7538)$, respectively. In addition, we can compute $c_1(\tau_0^0 \approx 5.7754) \approx -0.5467 - 1.6623$ and $c_1(\tau_1^0 \approx 19.9272) \approx 0.1087 - 0.8438$. From the discussions in Section 4, we know that the spatially homogeneous periodic solutions are stable on the center manifold and the inhomogeneous periodic solutions are unstable; see Figures 2 and 3.

We further perform some numerical computations. Let $\Delta x = \frac{\pi}{100}$ and $\Delta t = 0.05$ be the mesh size of x-direction and t-direction, respectively. The numerical solution is then denoted by $U_{\mathbf{j}}^{\mathbf{n}} \approx u(x_{\mathbf{j}}, t_{\mathbf{n}})$ and $V_{\mathbf{j}}^{\mathbf{n}} \approx v(x_{\mathbf{j}}, t_{\mathbf{n}})$; here, $x_{\mathbf{j}} = \mathbf{j}\Delta x$, $t_{\mathbf{n}} = \mathbf{n}\Delta t$, $\mathbf{j} = 0, 1, \ldots, 200$, $\mathbf{n} = 1, 2, 3, \ldots$. Let $\tau = 5.3$, and we choose a special mesh point of x-direction $x_{100} = 100\Delta x = \pi$. By using implicit difference scheme, numerical simulations at $x_{100} = \pi$ and numerical solutions $U_{100}^{\mathbf{n}}$ and $V_{100}^{\mathbf{n}}$ when $\mathbf{n} = 40\mathbf{k}$ ($\mathbf{k} = 1, 2, \ldots, 25$) are given in Figure 4 and Tables 2 and 3, respectively, which illustrate the asymptotic stability of $(1.6462, 0.7538)$ located in $x_{100} = \pi$. When $\tau = 6.2 > \tau_0^0 \approx 5.7754$, numerical simulations at $x_{100} = \pi$ and numerical solutions $U_{100}^{\mathbf{n}}$ and $V_{100}^{\mathbf{n}}$ with $\mathbf{n} = 10\mathbf{k}$ ($\mathbf{k} = 119, 120, \ldots, 160$) are presented in Figure 5 and Tables 4 and 5, which show that system (2) bifurcates a periodic solution near $(1.6462, 0.7538)$ located in $x_{100} = \pi$.

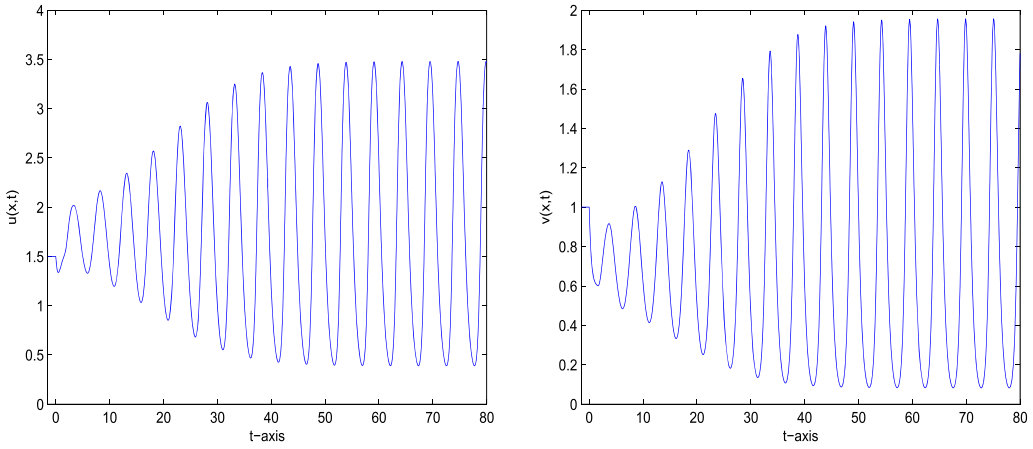

FIGURE 5 Numerical simulations of system (2) with the parameters given in Example 1 at mesh point $x_{100} = \pi$ plotted against $t_{\mathbf{n}} = \mathbf{n}\Delta t$ with $\tau = 6.2$ [Colour figure can be viewed at wileyonlinelibrary.com]

TABLE 5 The numerical solution $V_{100}^{\mathbf{n}}$ when $\mathbf{n} = 10\mathbf{k}$ ($\mathbf{k} = 119, 120, \ldots, 160$)

Solution	1190	1200	1210	1220	1230	1240	1250
$V_{100}^{\mathbf{n}}$	2.0075	1.5863	0.9167	0.4672	0.2459	0.1555	0.1390
Solution	1260	1270	1280	1290	1300	1310	1320
$V_{100}^{\mathbf{n}}$	0.2078	0.4905	1.2004	1.9343	1.8336	1.1702	0.6149
Solution	1330	1340	1350	1360	1370	1380	1390
$V_{100}^{\mathbf{n}}$	0.3134	0.1808	0.1376	0.1651	0.3355	0.8629	1.7060
Solution	1400	1410	1420	1430	1440	1450	1460
$V_{100}^{\mathbf{n}}$	1.9867	1.4501	0.8063	0.4081	0.2200	0.1468	0.1436
Solution	1470	1480	1490	1500	1510	1520	1530
$V_{100}^{\mathbf{n}}$	0.2390	0.5923	1.3749	1.9925	1.7216	1.0418	0.5373
Solution	1540	1550	1560	1570	1580	1590	1600
$V_{100}^{\mathbf{n}}$	0.2772	0.1667	0.1366	0.1823	0.4019	1.0206	1.8344

6 | CONCLUSION

In this paper, we have studied spatiotemporal dynamic patterns of a reaction-diffusion predator-prey model with IGP. We revealed the effects of time delay and cross-fractional diffusion on our model. By taking time delay as the bifurcation parameter and analyzing the characteristic equation of the linearized system of the model at the positive constant steady state, the asymptotic stability of positive constant steady state is investigated and the existence of Hopf bifurcation occurring at the positive constant steady state is demonstrated. The results showed that the positive constant steady state is asymptotically stable when discrete delay is less than a certain critical value and unstable when the discrete delay is greater than this critical value, and the model can exhibit a Hopf bifurcation at the positive constant steady state when the discrete delay crosses through the above critical value. In addition, by using the normal form theory and the center manifold argument to PFDEs, the explicit formulae determining the properties of Hopf bifurcation such as the direction of Hopf bifurcation, the stability, and period of the bifurcated periodic solutions are given. When proper cross-fractional diffusion terms are introduced in the model, the Turing pattern emerged when cross-fractional diffusion coefficient d_{12} and d_{21} falls into some domain. Numerical simulations showed that the smaller order of fractional diffusion is, the more easily Turing pattern is able to occur. It will be interesting to consider the existence of stationary solution (ie, nonconstant positive steady state) of system (4), and we will further focus on this problem in forthcoming research.

ACKNOWLEDGEMENTS

Z.-P. Ma was supported by the National Natural Science Foundation of China (11761059) and by the Institutions of Higher Learning Scientific Research Project of Henan Province of China (15A110002). H.-F. Huo and H. Xiang were supported by the National Natural Science Foundation of China (11861044 and 11661050) and the HongLiu first-class disciplines Development Program of Lanzhou University of Technology.

CONFLICT OF INTEREST

This work does not have any conflicts of interest.

ORCID

Hai-Feng Huo https://orcid.org/0000-0002-9563-1483

REFERENCES

1. Pimm SL, Lawton JH. On feeding on more than one trophic level. *Nature*. 1978;275:542-544.
2. Polis GA, Myers CA, Holt RD. The ecology and evolution of intraguild predation: potential competitors that eat each other. *Ann Rev Ecol Syst*. 1989;20:297-330.
3. Arim M, Marquet PA. Intraguild predation: a widespread interaction related to species biology. *Ecol Lett*. 2004;7:557-564.
4. Hall RJ. Intraguild predation in the presence of a shared natural enemy. *Ecology*. 2011;92:352-361.
5. Polis GA, Holt RD. Intraguild predation: the dynamics of complex trophic interactions. *Trends Ecol Evol*. 1992;7:151-154.
6. Fang L, Wang J. The global stability and pattern formations of a predator-prey system with consuming resource. *Appl Math Lett*. 2016;58:490-55.
7. Shu H, Hu X, Wang L, Watmough J. Delay induced stability switch, multitype bistability and chaos in an intraguild predation model. *J Math Biol*. 2015;71:1269-1298.
8. Holt RD, Polis GA. A theoretical framework for intraguild predation. *Amer Nat*. 1997;149:745-764.
9. Fan G, Wolkowicz GSK. A predator-prey model in the chemostat with time delay. *Int J Differ Equ*. https://doi.org/10.1155/2010/287969
10. Li MY, Lin X, Wang H. Global Hopf branches and multiple limit cycles in a delayed Lotka-Volterra predator-prey model. *Discrete Contin Dyn Syst Ser B*. 2014;19:747-760.
11. Ruan S. On nonlinear dynamics of predator-prey models with discrete delay. *Math Mod Nat Phen*. 2009;4:140-188.
12. Shi J. Absolute stability and conditional stability in general delayed differential equations. In: Advances in Interdisciplinary Mathematical Research, Springer Proc. Math. Stat. Springer; 2013; New York.
13. Wolkowicz GSK, Xia H. Global asymptotic behavior of a chemostat model with discrete delays. *SIAM J Appl Math*. 1997;57:1019-1043.
14. Wu J. *Theory and Applications of Partial Functional Differential Equations*. New York: Springer-Verlag; 1996.
15. Chen X, Du Z. Existence of positive periodic solutions for a neutral delay predator-prey model with Hassell-Varley type functional response and impulse. *Qual Theory Dyn Syst*. 2017. https://doi.org/10.1007/s12346-017-0223-6
16. Chen Z, Li F. Positive periodic solutions for a kind of second-order neutral differential equations with variable coefficient and delay. *Mediterr J Math*. 2018;15:19.
17. Huo HF, Jing SL, Wang XY, Xiang H. Modelling and analysis of an alcoholism model with treatment and effect of twitter. *Math Biosci Eng*. 2019;16:3595-3622.
18. Xiang H, Wang YY, Huo HF. Analysis of the binge drinking models with demographics and nonlinear infectivity on networks. *J Appl Anal Comput*. 2018;8:1535-1554.
19. Xiang H, Zou MX, Huo HF. Modeling the effects of health education and early therapy on tuberculosis transmission dynamics. *Int J Nonlinear Sci Number Sim*. 2019;20:243-255.
20. Huo HF, Yang Q, Xiang H. Dynamics of an edge-based SEIR model for sexually transmitted diseases. *Math Biosci Eng*. 2020;17:669-699.
21. Song Y, Jiang H, Liu Q, Yuan Y. Spatiotemporal dynamics of the diffusive mussel-algae model near Turing-Hopf bifurcation. *SIAM J Appl Dyn Syst*. 2017;16:2030-2062.
22. Huang S, Tian Q. Marcinkiewicz estimates for solution to fractional elliptic Laplacian equation. *Comput Math Appl*. 2019;78:1732-1738.
23. Huang S. Quasilinear elliptic equations with exponential nonlinearity and measure data. *Math Method Appl Sci*. 2020. https://doi.org/10.1002/mma.6088
24. Meng XY, Li J. Stability and Hopf bifurcation analysis of a delayed phytoplankton-zooplankton model with Allee effect and linear harvesting. *Math Biosci Eng*. 2020;17:1973-2002.
25. Wang J, Wei J, Shi J. Global bifurcation analysis and pattern formation in homogeneous diffusive predator-prey systems. *J Differential Equations*. 2016;260:3495-3523.
26. Xiang H, Tang YL, Huo HF. A viral model with intracellular delay and humoral immunity. *Bull Malays Math Sci Soc*. 2017;40:1011-1023.
27. Xing Y, Zhang L, Wang X. Modelling and stability of epidemic model with free-living pathogens growing in the environment. *J Appl Anal Comput*. 2020;10:55-70.
28. Turing A. The chemical basis of morphogenesis. *Philos Trans R Soc Ser B*. 1952;237:37-72.
29. Castets V, Dulos E, Boissonade J, Kepper PD. Experimental evidence of a sustained Turing-type equilibrium chemical pattern. *Phys Rev Lett*. 1990;64:2953-2956.
30. Kepper PD, Castets V, Dulos E, Boissonade J. Turing-type chemical patterns in the chlorite-iodide-malonic acid reaction. *Physica D*. 1991;49:161-169.
31. Solomon TH, Weeks ER, Swinney H. Observation of anomalous diffusion and Lévy flights in a two-dimensional rotating flow. *Phys Rev Lett*. 1993;71:3975-3978.
32. Zanette DH. Wave fronts in bistable reactions with anomalous Lévy-flight diffusion. *Phys Rev E*. 1997;55:1181.

33. Schmitt FG, Seuront L. Multifractal random walk in copepod behavior. *Phys A*. 2001;301:375-396.
34. Toner J, Tu Y, Ramaswamy S. Hydrodynamics and phases of flocks. *Ann Phys*. 2005;318:170-244.
35. Viswanathan GM, Afanasyevt V, Buldyrev SV, et al. Lévy flight search patterns of wandering albatrosses. *Nature*. 1996;381:413-415.
36. Ruan S. Absolute stability, conditional stability and bifurcation in Kolmogorov-type predator-prey systems with discrete delays. *Quart Appl Math*. 2001;59:159-173.
37. Ruan S, Wei J. On the zeros of a third degree exponential polynomial with applications to a delayed model for the control of testosterone secretion. *IMA J Math Appl Med Biol*. 2001;18:41-52.
38. Hassard B, Kazarinoff N, Wan Y. *Theory and Applications of Hopf Bifurcation*. Cambridge: Cambridge Univ. Press; 1981.

How to cite this article: Ma Z-P, Huo H-F, Xiang H. Spatiotemporal patterns induced by delay and cross-fractional diffusion in a predator-prey model describing intraguild predation. *Math Meth Appl Sci*. 2020;43:5179-5196. https://doi.org/10.1002/mma.6259